UNIVERSITÀ DEGLI STUDI DI PALERMO

Meccanica dei Materiali e delle Strutture
Vol. 3 (2012), no.2, pp. 25-32
ISSN: 2035-679X
Dipartimento di Ingegneria Civile, Ambientale, Aerospaziale, Dei Materiali
DICAM

DETECTION OF CRUSTAL MOVEMENTS FOR THE 2011 TOHOKU, JAPAN EARTHQUAKE FROM MULTI-TEMPORAL HIGH-RESOLUTION SAR INTENSITY IMAGES

Fumio Yamazaki[*], Wen Liu[†]

[*] Graduate School of Engineering, Chiba University
1-33, Yayoi-cyo, Inage-ku, Chiba 263-8522, Japan
e-mail: fumio.yamazaki@faculty.chiba-u.jp

[†]Graduate School of Engineering, Chiba University
1-33, Yayoi-cyo, Inage-ku, Chiba 263-8522, Japan
e-mail: wen_liu@graduate.chiba-u.jp

(Ricevuto10 Giugno 2012, Accettato 10 Ottobre 2012)

Key words: Crustal movement, TerraSAR-X, 2012 Tohoku earthquake, GPS.

Abstract. *Significant crustal movements were caused by the 2011 Tohoku, Japan earthquake. A method for capturing the surface movements from TerraSAR-X intensity images is proposed in this study. First, the buildings were extracted from the pre- and post-event SAR images using a segmentation approach. Then, the unchanged buildings were detected by matching the buildings in the pre- and post-event images at similar locations. Finally, the shifts were calculated and considered as crustal movements. The method was tested and its result was compared with GPS observation records. The proposed method was found to be able to detect crustal movement at a subpixel level.*

1 INTRODUCTION

The Mw 9.0 Tohoku earthquake, which occurred on March 11, 2011, off the Pacific coast of northeastern (Tohoku) Japan, caused gigantic tsunamis, resulting in widespread devastation. The epicenter was located at 38.322° N, 142.369° E at a depth of about 32 km. The earthquake resulted from a thrust fault on the subduction zone plate boundary between the Pacific and North American plates. According to the GPS Earth Observation Network System (GEONET) at the Geospatial Information Authority (GSI) in Japan, crustal movements with maximums of 5.3 m in the horizontal (southeast) and 1.2 m in the vertical (downward) directions were observed over a wide area [1]. Although GSI has established about 1,200 GPS ground control stations throughout Japan, the distance between two neighboring stations is over 20 km. Hence, it remains difficult to capture a detailed crustal movement distribution using only GPS recording data. Also developing countries are unable to establish GPS recording systems. Thus, measuring crustal movements estimated from satellite data constitutes an efficient and important method.

Two methods have normally been used to detect crustal movements in remote sensing images in past studies. The first is interferometric analysis of synthetic aperture radar (SAR) [2]. Several studies have been conducted to detect displacements due to earthquakes based on differential SAR interferometry (DInSAR) [3, 4]. However, depending on vegetation and temporal decorrelation [5], InSAR may not always be able to measure ubiquitous deformation at a large scale. The second method is the pixel-offset method, which can be applied to both SAR and optical images. Michel et al. [6] and Tobita et al. [7] measured ground displacements after earthquakes using SAR amplitude images. Crippen [8], Leprince et al. [9], and González et al. [10] also detected ground deformation in SPOT and IRS panchromatic imagery. Using the method, two images are coregistered for non-displaced boundaries, before internal local deformation is calculated by cross-correlation. 3D surface displacement estimates have been obtained by InSAR and pixel-offset methods using GPS records and SAR image pairs captured from ascending and descending orbits [11-13].

In the 2011 Tohoku earthquake, the extent of crustal movements was much larger than the SAR imaging area. Due to the absence of the accurate geocoding information, it was difficult to detect the absolute displacement using the previous methods. The high-accuracy georeferenced product, however, has become available recently due to the improvement of SAR sensors and thus we used it to estimate the absolute ground displacements even in the case of large-scale tectonic movements.

In this study, pre- and post-event TerraSAR-X (TSX) intensity images from the Tohoku earthquake were used to detect crustal movements based on the shifts of unchanged buildings. The accuracy of the proposed method was demonstrated by comparing the detected displacements with those from GPS ground station records.

2 STUDY AREA AND IMAGE PREPROCESSING

The study area was focused on the coastal zone of Tohoku, Japan, as shown in Fig. 1(a), which was one of the most severely affected areas during the 2011 Tohoku earthquake. Two temporal TSX images taken before and after the earthquake are shown in Fig. 1(b-c), which we used for detecting crustal movements. The pre-event image was taken on October 26, 2010 (UTC) while the post-event ones were taken on March 18, 2011. There is a 21.47° incident angle at the center of the images. Two images were captured with horizontal transmit and horizontal receive (HH) polarization and in a descending path. The images were acquired in the StripMap mode, and thus the azimuth resolution and the ground range resolution were about 3.1 × 3.5 m. We used Enhanced Ellipsoid Corrected (EEC) products of processing level 1B, where the image distortion caused by a variable terrain height was compensated for by using a globally available digital elevation model (SRTM). The products were provided in the form projected to a World Geodetic System 84 reference ellipsoid with a resampled square pixel size of 1.25 m.

Two preprocessing approaches were applied to the images before extracting crustal movements. First, the two TSX images were transformed to a Sigma Naught (σ_0) value,

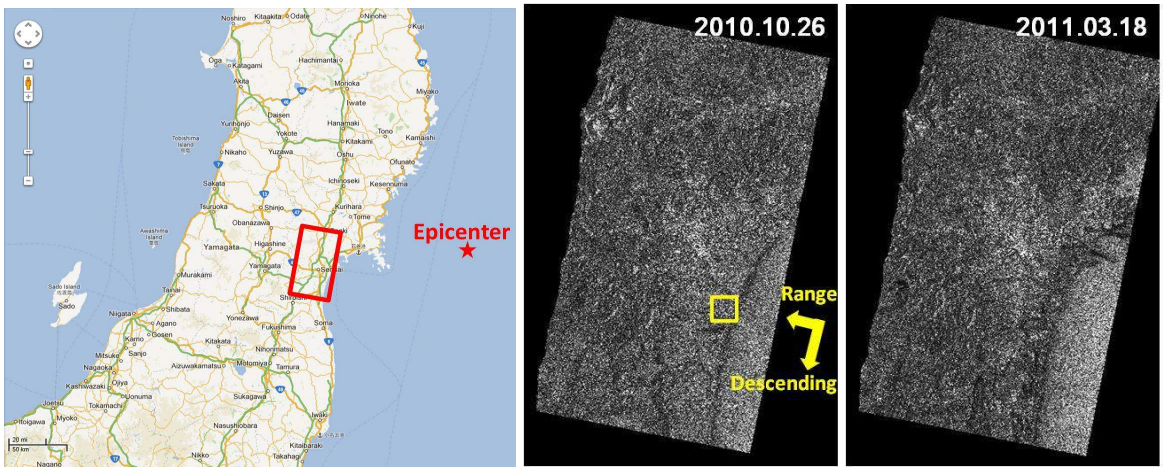

(a) (b) (c)

Figure 1: Study area on the Pacific coast of Tohoku, Japan (a); the pre-event TSX image taken on October 26, 2010 (b); and the post-event images taken on March 18, 2011 (c).

which represents the radar reflectivity per unit area in the ground range. An Enhanced Lee filter was then applied to the original SAR images to reduce the speckle noise. To minimize any loss of information included in the intensity images, the window size of the filter was set as 3 × 3 pixels. The pixel localization corrected by the GPS orbit determination was used directly in this study. According to the product specification document [14], the pixel localization accuracy of EEC products depends on the orbit and the DEM used. Since the four EEC products were made using the same DEM following the same process, the errors caused by DEM were cancelled out when comparing two images. Since the orbit type of our TSX images was "Science", their required orbit accuracy is within 20 cm [15].

3 METHODOLOG

This study proposes a method for detecting crustal movements based on the measurement of the movements of unchanged buildings in SAR intensity images. In current methods, crustal movements are usually detected by registering ground surface. However, during the Tohoku earthquake, a gigantic tsunami hit many cities/towns along the coast and the ground surface was changed significantly by debris or flooded seawater. Thus, our study focused on the movements of unchanged buildings to ensure a stable correlation and highly accurate movement detection. First, segmentation was performed on both images to extract the location of building objects. Next, matching was introduced to detect unchanged buildings. The displacements of unchanged buildings were calculated using an area-based matching method. Finally, all the movements of unchanged buildings were obtained, and they were considered to be the crustal movements in the study area.

3.1 Segmentation and extraction

In most cases, buildings show a higher backscatter than other surface objects in SAR images because of their corner reflection. To detect the locations of buildings, we performed segmentation on the pre- and post-event TSX images. According to a visual inspection of the histograms of the SAR images, the threshold value of the backscattering coefficient between buildings and other objects was set e as –2.0 dB. Based on a typical building size, only objects larger than 100 pixels (about 150 m^2) were extracted as engineered (solid) buildings. Thus,

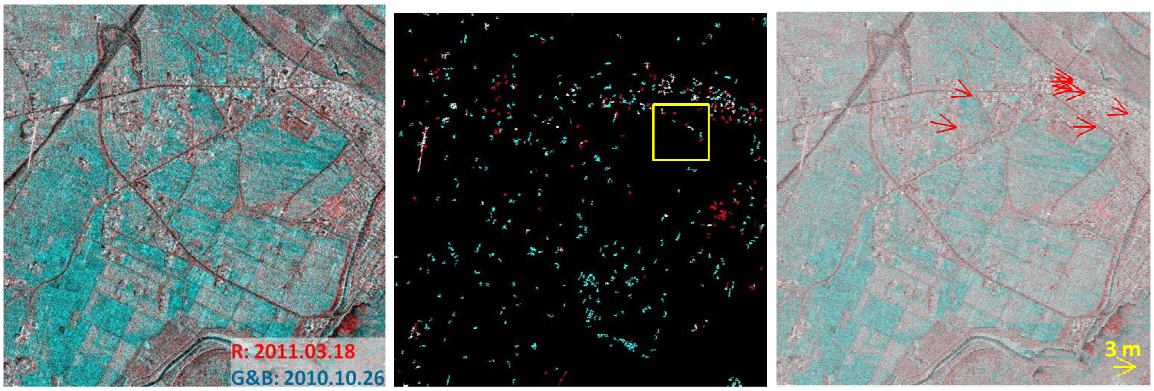

(a) (b) (c)

Figure 2: Color composit of pre- and post-event TSX image (a) and building images (b) within the yellow frame in Fig. 1(b); detected results showing the displacement vectors overlapping on the color composite image.

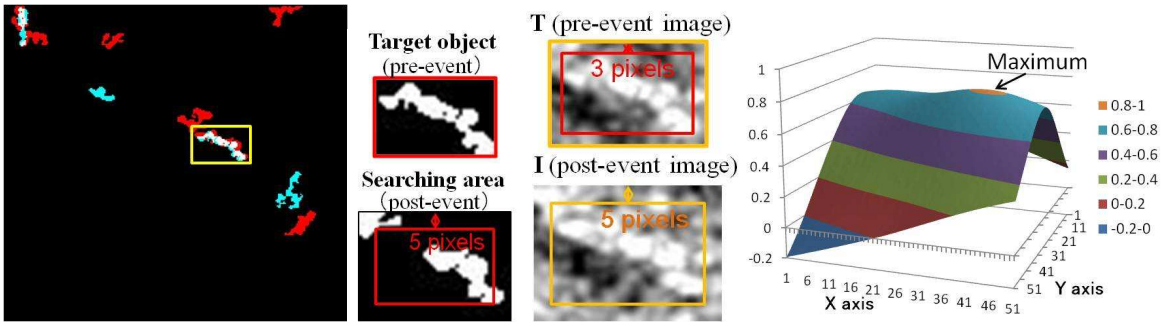

(a) (b) (c) (d)

Figure 3: A pick-up of the area in the yellow frame of Fig. 2(b) (a); a target building object in the pre-event and the search area in the post-event building image (b); target area T in the pre-event SAR image and the search area I surrounding the target area in the post-event image (c), and similarity matrix for them (d).

objects with an average backscattering coefficient greater than –2.0 dB and larger than 100 pixels were extracted and used in the next step. A part of the color composition of the pre- and post-event is shown in Fig. 2(a), and the building image is shown in Fig. 2(b). From the pick-up of the building image shown in Fig. 3(a), obvious shifts can be seen in the shapes of the same buildings between images.

The tsunami caused by the earthquake affected vast amounts of coastal areas, and many constructions such as wooden houses and seawalls were destroyed or carried away. Thus, the shifts of unchanged buildings had to be observed to measure the crustal movements. A building object extracted from the pre-event building image was selected as a target object. A rectangular area surrounding the target building and exceeding its size was then selected from the post-event building image as the search area. An example of the target and search areas is shown in Fig. 3(b). If a building object existed in this area, then the target building was considered as unchanged. Based on the GPS ground control points data, the maximum crustal movement observed during this earthquake was about 5.3 m, and thus the search area was set as 5 pixels (6.25 m) larger than the target object in every direction.

3.2 Calculation of movements

After detecting the locations of unchanged buildings, the shifts of building shapes due to the earthquake were calculated using an area-based method. The target area (T) was selected from the pre-event intensity image in the locations of unchanged building objects, which were extracted in the previous step. To improve the accuracy of area-based matching, the ground

surface surrounding the building object within a distance of 3 pixels was also included in the target area. The search area (I) was selected in the post-event intensity image, which surrounded the target area and exceeded it in size. Examples of T and I are shown in Fig. 3(c). The target and search areas were resampled to 0.25 m/pixel by cubic convolution to 1/5 of the original pixel size. The shift of building shapes could then be detected at a sub-pixel level.

Area correlation is a method used for designating GCPs during image-to-image registration. In this study, the target area was overlaid with the search area and a similarity index was calculated. The similarity matrix contained the values of the statistical comparison between the target and search areas. The position in the similarity matrix where the similarity index reached a maximum value represented the necessary offset that the target had to move along the x- and y-axes to match the searching area.

An example of a calculated similarity matrix is shown in Fig. 3(d). The target and search areas were selected with the same center point, and hence the maximum value should be at the center of the matrix if no movement occurred. In this case, the building moved 3.00 m to the east. The vectors of movements which were detected from the image Fig. 2(a) are shown in Fig. 2(c).

4 RESULTS AND VERIFICATION

The TSX images in the red frame of Fig. 4(a) were divided into a square mesh containing 4000 × 4000 pixels (5 × 5 km2), to detect the ground movements. The target area includes 5 GPS stations, named Miyagi-daiwa, Rifu, Sendai, Natori and Watari. The movements of unchanged buildings were calculated in each sub-area and the average value was considered to be the crustal movement of the sub-area. To ensure that the pre-event building matched with the same post-event building correctly, only the shift of a building with a similarity index higher than 0.8 was counted as valid. Additionally, only a sub-area containing more than 5 building displacements was counted as a valid sub-area to achieve the reliability of the results.

4.1 Results

There were 69 sub-areas within the target area, and crustal movements were detected successfully from 46 sub-areas. The displacement vectors throughout the image are shown in Fig. 4(b). Since northwestern areas were mountainous with less buildings, the crustal movement could not be detected. The sub-area near the coast including Natori GPS station was severally affected by tsunami. Therefore there were only 8 buildings with high similarity indexes and counted as invalid.

The distance map is shown in Fig. 4(c) with rainbow color. The detected movements were between 2 and 3 m. The largest movement occurred in a northeastern area which is nearer to the epicenter, and it got smaller when moving southwards. The angular heading of the detected movements moved close to the east when heading southwards. These trends matched with the observed GPS data at ground stations. The detected amplitude and direction of crustal movements in the sub-areas which include the ground stations are shown in Table 1.

4.2 Verification

To verify the accuracy and usefulness of the proposed method, we compared the detected results with the crustal movement data at GPS stations. Surface deformation is a vector in three-dimensional space with three components, DE, DN, and DZ, in the east, north, and vertical directions, respectively. The relationship between an actual crustal movement and its

Location	Miyagi-daiwa		Rifu		Sendai		Natori		Watari	
Number of buildings	19		51		15		8		46	
	East	North	East	North	East	North	East	North	East	North
TSX	2.39	-0.68	2.66	-0.64	2.55	-0.62	2.75	-0.47	2.52	-0.33
GPS records	2.43	-0.69	2.52	-0.68	2.32	-0.52	□	□	2.33	-0.40

Table 1: Detected crustal movements in five sub-areas surrounding the GPS stations between Oct. 26, 2010 and March 18, 2011 (unit: meter).

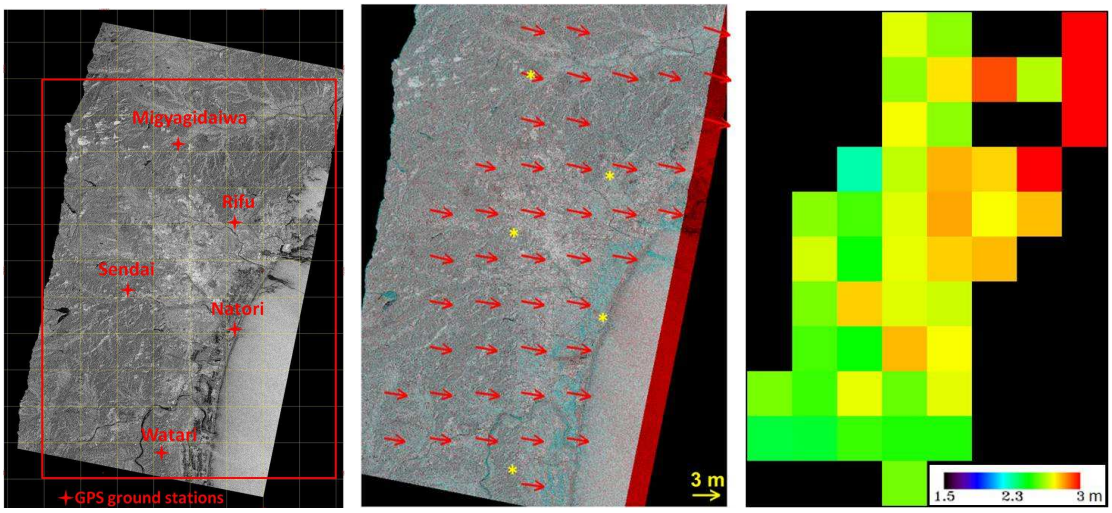

(a) (b) (c)

Figure 4: Target area including 5 GPS ground station was indived into 5 x 5 km^2 sub-areas (a); the detected displacement vectors in each sub-area in the periods of October 26, 2010 to March 18, 2011 overlapping on the color composite of the TSX intensity images (b), and the displacement amplitude values shown in rainbow color (c).

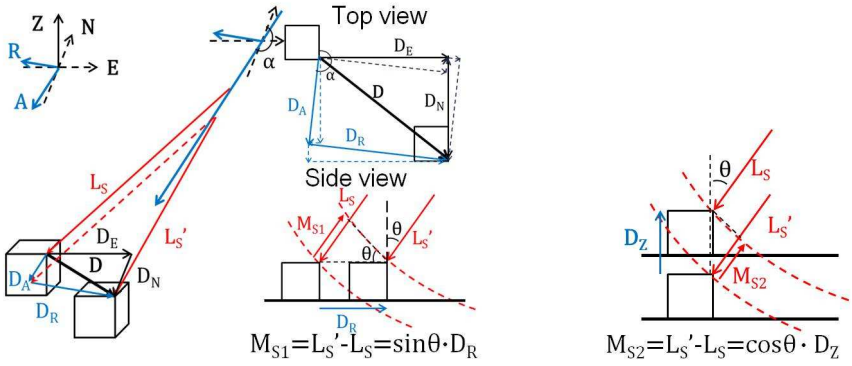

(a) (b)

Figure 5: Schematic views of the horizontal (a) and vertical displacements (b) in a SAR image.

shift in a SAR image is shown in Fig. 5. SAR intensity images are geocoded with a spacing to the north and east directions. Hence the relationship between a crustal movement (*D*) and its shift (*M*) in a ground range SAR image can be described using Eq. (1).

$$\begin{pmatrix} M_E \\ M_N \end{pmatrix} = \begin{pmatrix} 1 & 0 & \cos\alpha / \tan\theta \\ 0 & 1 & \sin\alpha / \tan\theta \end{pmatrix} \begin{pmatrix} D_E \\ D_N \\ D_Z \end{pmatrix} \quad (1)$$

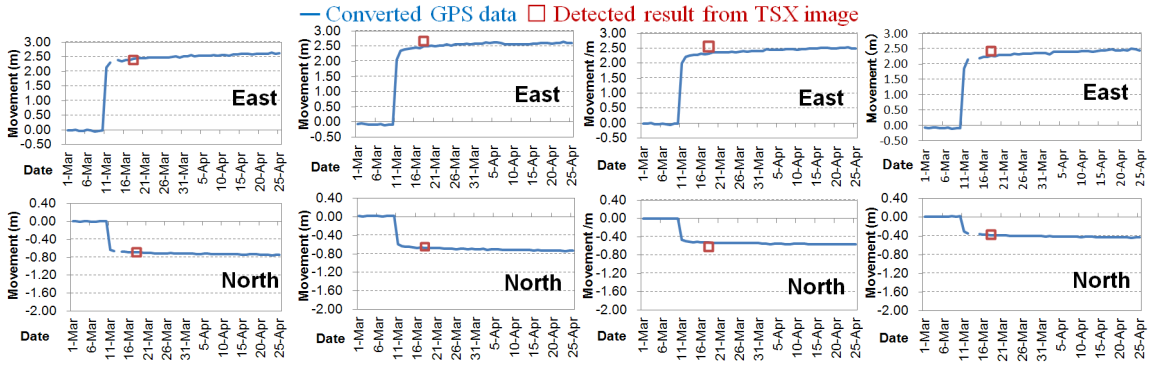

(a) Miyagi-daiwa (b) Rifu (c) Sendai (d) Watari

Figure 6: Comparison of movements converted from GPS data at Miyagi-daiwa (a), Rifu (b), Sendai (c), and Watari (d) ground control stations and the results detected in surrounding 25 km^2 sub-areas.

where *D* is the actual movement in the east, north, and vertical directions; *M* is the shift in the SAR image; α is the heading angle clockwise from north; and θ is the SAR incident angle.

The GPS recordings made at Miyagi-daiwa Rifu, Sendai and Watari stations from March 1 to April 25, 2011, were converted using Eq. (1) with a heading angle of 19.3° and a 37.4° incident angle, as shown in Table 1. Miyagi-daiwa and Watari stations stopped after the earthquake due to power outage and/or strong shaking. Natori station was the most seriously damaged and it did not restart until April 18, 2011. The measurement of ground movements in satellite images provides an important and effective tool in such cases. A comparison of the results detected around a GPS station with the converted GPS recording demonstrated a very high level of consistency, which is shown in Fig. 6. Based on 4 comparison points, the averaged differences between the detected result and the GPS measurement were about 0.1 m to the east and to the north respectively.

5 CONCLUSIONS

In this study, we proposed a method for detecting crustal movements due to a major earthquake on the basis of a comparison between two temporal SAR intensity images. The method was tested using two TerraSAR-X images covering the coast of Miyagi Prefecture, Japan before and after the 2011 Tohoku earthquake, which is a very difficult case as the displacement exceeded the image area. Although it is impossible to detect the actual 3D movement only from the descending pair, the four sub-areas surrounding GPS stations exhibited stable shifts of unchanged buildings and similar to the converted observed GPS data. Subpixel-based matching made it possible to detect movements with high accuracy, within 0.2 m. However, the accuracy of our method depends on the location accuracy of the original SAR images. Although the results obtained in this study are promising, we will further test the proposed method for other events including smaller surface displacements to validate its applicability. A further study will be carried out to enhance the proposed method to 3D cases.

ACKNOWLEDGEMENTS

The TerraSAR-X images used in this study were provided by Pasco Corporation, Tokyo, Japan, as one of the funded projects of the SAR Data Application Research Committee.

REFERENCES

[1] Geospatial information Authority of Japan, available: http://www.gsi.go.jp/BOUSAI/h23_tohoku.html#namelink3.

[2] H.A. Zebker, "Studying the Earth with interferometric radar", *IEEE Computing in Science & Engineering*, **2**(3), 52-60 (2000).

[3] S. Stramondo, F.R. Cinti, M. Dragoni, S. Salvi and S. Santini, "The August 17, 1999 Izmit, Turkey, earthquake: Slip distribution from dislocation modeling of DInSAR and surface offset", *Annals of Geophysics*, **45**(3/4), 527-536 (2002).

[4] M. Chini, S. Atzori, E. Trasatti, C. Bignami, C. Kyriakopoulos, C. Tolomei and S. Stramondo, "The May 12, 2008, (Mw 7.9) Sichuan Earthquake (China): Multiframe ALOS-PALSAR DInSAR Analysis of Coseismic Deformation", *IEEE Geoscience and Remote Sensing Letters*, **7**(2), 266-270 (2010).

[5] R. Bürgmann, P. A. Rosen and E. J. Fielding, "Synthetic Aperture Radar interferometry to measure earth's surface topography and its deformation", *Annual Reviews Earth and Planet Sciences*, **28**, 169-209 (2000).

[6] R. Michel, J.-P. Avouac and J. Taboury, "Measuring ground displacements from SAR amplitude image: application to the Landers earthquake", *IEEE Geophysical Research Letters*, **26**(27), 875-878 (1999).

[7] M. Tobita, H. Suito, T. Imakiire, M. Kato, S. Fujiwara and M. Murakami, "Outline of vertical displacement of the 2004 and 2005 Sumatra earthquakes revealed by satellite radar imagery", *Earth Planets Space*, **48**(1), e1-e4 (2006).

[8] R. E. Crippen, "Measurement of sub resolution terrain displacements using SPOT panchromatic imagery", *International Journal of Remote Sensing*, **15**(1), 56-61 (1992).

[9] S. Leprince, S. Barbot, F. Ayoub and J.-P. Avouac, "Automatic and precise orthorectification, coregistration, and subpixel correlation of satellite images, Application to ground deformation measurements." *IEEE Trans. on Geos. Remote Sensing*, **45**(6): 1529-1558 (2007).

[10] P. J. González, M. Chini, S. Stramondo and J. Fernández, "Coseismic horizontal offsets and fault-trace mapping using phase correlation of IRS satellite images: The 1999 Izmit (Turkey) Earthquake", *IEEE Trans. on Geos. Remote Sensing*, **48**(5), 2242-2250 (2010).

[11] Y. Fialko, M. Simons and D. Agnew, "The complete (3-D) surface displacement field in the epicentral area of the 1999 Mw7.1 Hector Mine earthquake, California, from space geodetic observations", *Geophysical Research Letters*, **28**(16): 3063-3066 (2001).

[12} J. Catalão, G. Nico, R. Hanssen and C. Catita, "Merging GPS and atmospherically corrected InSAR data to map 3-D terrain displacement velocity", *IEEE Trans. on Geos. Remote Sensing*, **49**(6): 2354-2360 (2011).

[13] M. de Michele, D. Raucoules, J. de Sigoyer and M. Pubellier, "Three dimensional surface displacement of the 2008 May 12 Sichuan earthquake (China) derived from Synthetic Aperture Radar: evidence for rupture on a blind thrust", *Geophysical Journal International* (2010).

[14] M. Eineder, T. Fritz, J. Mittermayer, A. Roth, E. Borner, H. Breit and B. Brautigam, "TerraSAR-X Ground Segment Basic Product Specification Document", TX-GS-DD-3302, Issue 1.7, 31-32 (2010).

[15] M. Wermuth, A. Hauschild, O. Montenbruck and A. Jäggi, "TerraSAR-X Rapid and Precise Orbit Determination", *21st International Symposium on Space Flight Dynamics* (2009).